RSC Advances

ROYAL SOCIETY OF CHEMISTRY

www.rsc.org/advances

Journal Name

RSCPublishing

COMMUNICATION

Ultrafast Synthesis of Nitrogen-Doped Carbon Dots via Neutralization Heat for Bioimaging and Sensing applications

Cite this: DOI: 10.1039/x0xx00000x

Received ooth January 2012,
Accepted ooth January 2012

DOI: 10.1039/x0xx00000x

www.rsc.org/

Xiao-Mi Wei,[a]† Yang Xu,[a]† Yu-Hao Li,[b] Xue-Bo Yin,[a]* and Xi-Wen He[a]

Ultrafast synthesis (within 2 min) of nitrogen-doped carbon dots was achieved using neutralization heat with glucose as precursor. The hydroxyl groups on dots' surface from glucose make them easy conjugation with boronic acid (BA). Dual enhancement of fluorescence was observed by nitrogen-doping with ethylenediamine and the conjugation with BA.

Carbon dots (Cdots) are a new type of carbon nanomaterials (CNMs) with sizes less than 10 nm. Quantum confinement endows Cdots size- and wavelength-dependent fluorescence and low photobleaching. [1, 2] Synthesis, fluorescence mechanism, and potential applications of Cdots have been studied, [3] but Cdots are still less explored than other CNMs. [4-8] Nitrogen-doped Cdots (N-Cdots) have attracted much attention, because of their improved fluorescence emissions. [1, 4, 9, 10] Various substances contained high nitrogen content were used as nitrogen precursors to prepare Cdots.[11-15] Bright and tuneable fluorescence with high quantum yield were achieved among these N-Cdots. Cdots can be prepared with top-down procedure [1, 2, 16-20] and bottom-up approach. [1, 2, 9] Graphite, [16] soot, [17] and carbonized products [18, 19] were used to prepare Cdots with top-down procedure. [1] Various molecular precursors were treated hydrothermally to obtain surface-passviated and/or heteroatom-doped Cdots with bottom-up approach. [1, 4, 9, 10] However, most of the preparation methods are time-consuming and/or require complex instruments. [4, 21-23]

Cdots have been used in the fields of bioimaging, optoelectronics, biosensing, and photocatalysis, because of their properties, such as low toxicities, less photo-bleaching and high biocompatibilities. [1, 2] The functionalization of Cdots is the key step to improve the recognition specificity. [24] Some biolables were conjugated with nanoparticles for imaging because of their specificity to biological tissue or species.[25] Fast and easy synthetic methods and simple functionalization strategies for Cdots may promote the developments and applications of Cdots.

Herein, we present an ultrafast one-step approach to prepare N-Cdots suitable for biological labelling, imaging and sensing applications, with neutralization reaction as heat source and glucose as precursor. Glucose was dissolved into ethylenediamine, and then phosphoric acid was added. Cdots was prepared via the dehydration and carbonization of glucose within 2 min. Ethylenediamine was the heat source, while it also served as the nitrogen source for preparing N-Cdots with improved fluorescence. Compared with strong acids and oxidants used previously,[1, 2, 16, 17] phosphoric acid has low volatility and corrosivity. To the best of our knowledge, this is the simplest and fastest method for preparing N-Cdots without the use of any complex instrumentation. Moreover, N-Cdots surface functionalized with boronic acid (BA) and its derivatives were reported for the first time. Dual enhancement of fluorescence for N-Cdots was observed by the nitrogen-doping with ethylenediamine and the conjugation with BA.

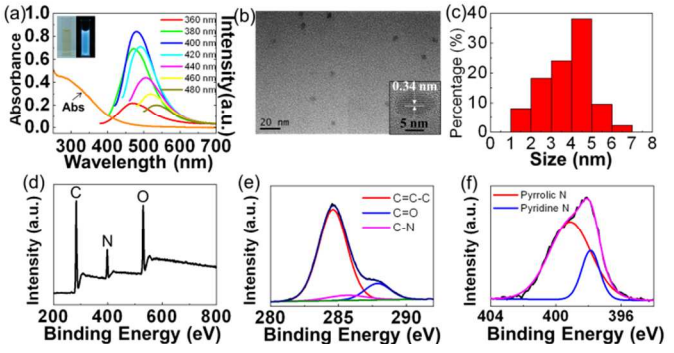

Fig. 1. (a) UV-vis spectra and excitation-dependent fluorescence spectra of N-Cdots. Inset: photographs of N-Cdots solutions (left) in sunlight and (right) under 365 nm excitation. (b) TEM image and high resolution TEM image (inset) of N-Cdots; (c) size distribution of N-Cdots obtained from TEM results; (d) XPS broad spectrum, (e) XPS C1s spectra, (f) XPS N1s spectra of N-Cdots.

Glucose was carbonized in 2 min with a 48 % yield of N-Cdots by the neutralization heat. The highest temperature was beyond 120 °C and maintained for at least 2 min, and then decreased gradually,

the same as the hydrothermal treatment of glucose at 120 °C to prepare Cdots. [26] However, high concentration of glucose accelerated its carbonization and promoted rapid nucleation over growth for preparation of N-Cdots with the high yield. [27, 28] Investigation of various bases illustrated that ethylenediamine not only served as the heat source for the synthesis of Cdots, but also served as the nitrogen source and passivation reagent for preparing N-Cdots (Fig. S1), as reported in previous work.[29] Because polyaromatic structures were produced by protonation of nitrogen atoms on Cdots,[12, 30] the use of ethylenediamine enhances the fluorescence of Cdots 10-fold comparing with the use of NaOH. The optimal ratio of glucose/ethylenediamine/phosphoric acid was confirmed to be 200 mg/15ml/8 ml (Fig. S1).

The N-Cdots were water-soluble and showed a yellow color, while a bright blue emission was observed when the N-Cdots were excited at 365 nm (inset in Fig. 1a). The N-Cdots have excitation-dependent emission behaviors (Fig. 1a), and show the multicolor properties, similar to those previously reported for Cdots. [10, 31-33] The emission peaks shifted from 470 to 540 nm in excitation range of 360-480 nm. The maximum emission was observed at 498 nm with the excitation at 400 nm. The absorption peak at 340 nm in UV-vis absorption spectra of N-Cdots confirmed the presence of aromatic π orbits, so carbonization occurs to form N-Cdots (Fig. 1a).

The size, morphology, and composition of N-Cdots were investigated. Transmission electron microscope (TEM) images showed that the N-Cdots had the size of 1–7 nm (Fig. 1b and 1c). The lattice fringes observed in the high resolution TEM images was 0.34 nm (inset in Fig. 1b), corresponding to the signal at $2\theta = 22°$ in X-ray diffraction (XRD) pattern (Fig. S2a). Some impurity peaks were observed in the XRD pattern because carbonization was incomplete and some residual groups from glucose remained on the N-Cdot surface. The broad peak at 3300 cm^{-1} in Fourier-transform infrared spectra showed the presence of hydroxyl and/or amino groups on the N-Cdots' surface (Fig. S2b). The peaks at 1630, 1450, and 1250 cm^{-1} were related to C=O, C=C and C-N stretching, indicating the formation of N-Cdots. In XPS spectra, pyridine- and pyrrolic-nitrogens were observed (Fig. 1d-1f). [34] Thus, nitrogen was successfully doped into the Cdots by the use of ethylenediamine.

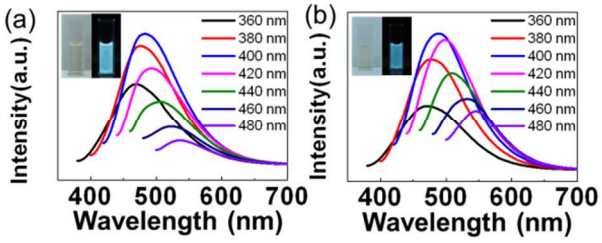

Fig. 2. Excitation-dependent fluorescence of Cdots prepared with (a) citric acid, and (b) sucrose as precursors. Inset: photos of Cdots solution in light and excited at 365 nm.

To investigate the generality of the synthesis method, sucrose and citric acid were used as carbon sources for the preparation of Cdots. The two precursors were also carbonized by neutralization heat to obtain Cdots; excitation-dependent emissions was observed with bright blue fluorescence under UV light (Fig. 2). The neutralization heat strategy is a versatile route for the fast synthesis of Cdots using the precursors. As shown in Fig. 1f, pyrrolic ring was found and formed by the reaction of precursors and ethylenediamine. The active hydroxyl groups in the semiacetal structure facilitate the formation of carbon core by inducing the intermolecular condensation of the precursors. [26] The carbonization and introduction of nitrogen therefore occurred simultaneously to form N-Cdots.

Some functional groups from glucose remain on the N-Cdot's surface as shown in XRD pattern because the reaction time and energy are inadequate for complete carbonization of glucose in 2 min. Thus, the reaction between N-Cdots and BA or phenylboronic acid (PBA) were investigated. BA or PBA enhanced the fluorescence of N-Cdots quickly through the interactions between adjacent hydroxyl and boronic groups. The specificity of the enhancement was confirmed by the other Cdots. The fluorescence of Cdots derived from citric acid by neutralization heat and that from hydrothermal treatment of glucose cannot enhance by BA or PBA (Fig. S3), so those Cdots cannot coordinate with BA or PBA because citric acid does not have adjacent hydroxyl group. The hydrothermal process lasted for 12 h to destroy the adjacent hydroxyl group structure for Cdots from glucose.

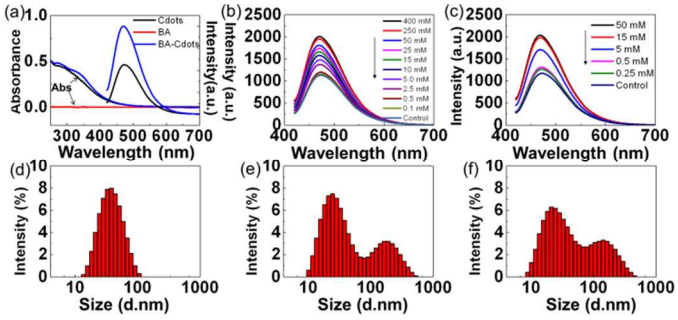

Fig. 3. (a) UV-vis and fluorescence spectra of N-Cdots, BA, and BA-modified N-Cdots. Fluorescence spectra of N-Cdots (0.05 mg mL^{-1}) treated with (b) BA and (c) PBA at different concentrations. The excitation wavelength was 400 nm. DLS distribution of (d) N-Cdots, (e) BA-Cdots and (f) PBA-Cdots.

The fluorescence enhancement was confirmed by the UV spectra of N-Cdots; the absorption intensities at 280 and 340 nm from N-Cdots increased after interacting with BA (Fig. 3a) although BA has no absorbance. The changed signal at 280 nm indicated that the number of sp^2 clusters in the N-Cdots increased. [35] The signal at 340 nm showed that the surface adsorption of N-Cdots was improved to enhance fluorescence emission, because this region contains the excitation wavelength. [9, 32] The adjacent hydroxyl groups on the N-Cdots surface provide the enhanced fluorescence emission via the interaction with BA, giving 1.78-fold improvement as shown in Fig. 3a.

The emission of N-Cdots was in concentration-dependent mode with BA or PBA (Fig. 3b, 3c, S4a, and S4b). Moreover, the fluorescence was enhanced quickly and reached its maximum in 2 min by BA (Fig. S4c). However, the fluorescence was enhanced slowly and slightly by PBA, possibly because of the steric hindrance (Fig. S4d). Dynamic light scattering (DLS) results further demonstrated the interactions with the increased size of N-Cdots after addition of BA or PBA (Fig. 3d-f). The DLS size of N-Cdots

ranged from 10–100 nm (Fig. 3d), larger than those observed in the TEM image (Fig. 2b) because of plenty of hydrophilic groups on the N-Cdots' surface. After addition of BA or PBA, new peak was observed because some of N-Cdots were conjugated with BA or PBA in Fig. 3e and 3f. The adjacent hydroxyl groups make N-Cdots easy functionalization for bio-label by simple incubation of the N-Cdots and BA-modified species.

Less photo-bleaching and high photo stability in salt solution were observed when the N-Cdots were illuminated with continuous UV light or in different concentrations of NaCl. The N-Cdots could be used for imaging with an illuminated time of 60 min without any decline in fluorescence (Fig. S5a), and the salt concentration could be up to 1 M NaCl (Fig. S5b). When stored in buffers at different pH, the fluorescence from the N-Cdots was stable in the pH range of 2–7 (Fig. S5c). Thus, the N-Cdots showed the potential for *in vivo* imaging and biosensing because of their stable emission.

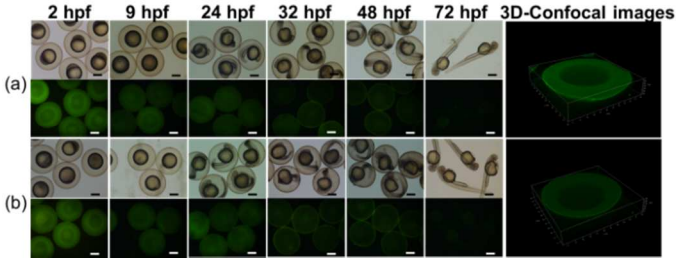

Fig. 4. (upper) Bright-field and (lower) fluorescence images of zebrafish embryo at different growing stages cultured with: (a) N-Cdots, (b) BA-Cdots at concentrations of 1.2 mg mL^{-1}. Three-dimensional confocal fluorescent images of zebrafish embryos at 2 hpf. Scale bar: 500 μm.

Zebrafish are widely used for fundamental research on pattern formation, developmental mechanism and disease progression, because of their well-defined developmental stage, emerging disease models, and their amenability to optical imaging. [36-40] Zebrafish embryonic development was used to examine the application of those Cdots for *in vivo* imaging. [34] The embryos were exposed to the solutions containing N-Cdots, and BA-Cdots, and PBA-Cdots for 2 h; the distributions of the Cdots were recorded at different growing stages of embryos. Compared with the control group, the Cdots-treated groups showed bright fluorescence at 24 hours post fertilization (hpf, Fig. 4). At 24–48 hpf, N-Cdots and BA-Cdots tended to attach to the chorions as the fluorescence on the edge of the embryos; the residual glucose units on the Cdot surfaces were specific to the chorion, where some glucose receptors exist. [41] The phenomenon was confirmed by the three-dimensional confocal fluorescence images at 2 hpf (Fig. 4). Moreover, the Cdots did not affect the embryonic development; the embryos underwent rapid cell division to form the organs from 32 to 48 hpf (Fig. S6). More than 80 % of zebrafish embryo viability was observed for the N-Cdots and BA-Cdots treated groups during the procedure, the same as the viability of 85 % of control group. N-Cdots and BA-Cdots therefore exhibited high biocompatibility and low toxicity for *in vivo* imaging to illustrate the embryonic development of zebrafish. However, PBA-Cdots are highly toxic and caused 100 % mortality of the embryos at 9 hpf (Fig. S7), indicating that PBA-Cdots and BA-Cdots have different biotoxicity. In vivo cytotoxicity study also showed that N-Cdots and BA-Cdots had the similar cell viabilities (Fig. S8). Although Cdots have been used for cellular imaging, [18] our work provided their distribution within an embryo and effects on embryonic development.[9, 42]

Ovalbumin is a monomeric pbosphoglycoprotein with high affinity to BA derivatives. [43] Ovalbumin was found in live rubella vaccine and can cause allergic reactions. [44] The fluorescence of PBA-Cdots and BA-Cdots was tested after addition of ovalbumin; the fluorescence of PBA-Cdots or BA-Cdots increased a little (Fig. S9). The enhanced fluorescence indicated the interaction between ovalbumin and PBA-Cdots or BA-Cdots. To build a turn-on biosensor for ovalbumin, graphene oxide (GO) first quenched the fluorescence of PBA-Cdots or BA-Cdots and then was recovered through the interaction of the modified Cdots and ovalbumin.

GO is the exfoliated product from graphite powder with abundant oxygen-containing groups. [45] Its highly quenching capability makes GO widely used as an energy transfer fluorescence quencher.[20-22] Various GO-based biosensors were used for detecting biomolecules, [46] small molecules, [47] and cations. [48] After PBA-Cdots or BA-Cdots were attached to GO through π–π stacking; their fluorescence was quenched significantly by GO in 10 s (Fig. S10). Then the biosensors were incubated with ovalbumin solution at different concentrations. Its affinity with PBA and BA makes ovalbumin closely approaches the Cdots, which were released from GO. The Cdots' fluorescence was recovered and the fluorescence intensity increased in a concentration-dependent mode (Fig. 5), so the systems could be used as effective turn-on biosensors. For PBA-Cdots/GO system, the linear range was 0.11–2.2 mg mL^{-1} with a correlation factor of 0.9927 for ovalbumin (Fig. 5c). The linear range was 0.022–1.76 mg mL^{-1} for BA-Cdots/GO biosensor with a correlation factor of 0.9928 and a detection limit of 8 μg mL^{-1} (Fig. 5d). The results in Fig. S11 illustrated the selectivity of PBA-Cdots/GO system for ovalbumin. Thus, the interaction of N-Cdots with BA and PBA provides additional selectivity.

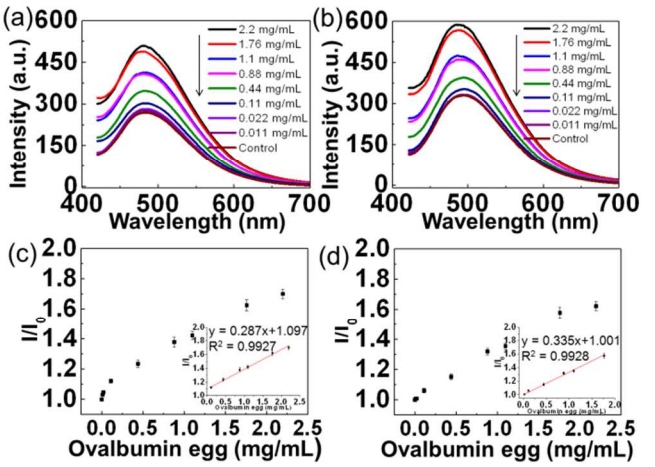

Fig.5. Fluorescence spectra of (a) GO/PBA-Cdots and (b) GO/BA-Cdots with ovalbumin at different concentrations. Concentration-dependent fluorescence intensities of (c) GO/PBA-Cdots and (d) GO/BA-Cdots solution in the presence of ovalbumin at different concentrations. Inset: linear calibration plot for ovalbumin detection. The concentrations of BA-Cdots and PBA-Cdots were 0.05 mg ml^{-1}, and that of GO was 0.01 mg ml^{-1}. Error bar represents the deviation of three repeated measurements. All

determinations were carried out in phosphate buffer solution (10 mM, pH 7.4) under excitation at 400 nm. I_0 is the fluorescence intensity of the control groups.

Conclusions

We proposed an ultrafast one-step approach for the preparation of blue-fluorescent N-Cdots. The method was time-saving, and no sophisticated instruments were required. As a result of rapid carbonization, some residual adjacent hydroxyl groups stayed on the N-Cdot surfaces and remained their original characteristics for surface functionalization of N-Cdots with BA and its derivatives. Dual enhancements of fluorescence from the N-Cdots were observed by the nitrogen-doping with the use of ethylenediamine and the conjugation with BA or PBA. Zebrafish embryos were used as a model to validate the potential for *in vivo* imaging of the N-Cdots. N-Cdots exhibited high biocompatibility and low toxicity to illustrate the embryonic development of zebrafish. A turn-on biosensor for ovalbumin was built through π–π stacking between PBA- or BA-Cdots and GO. This work provides a facile and fast method for N-Cdots preparation and the functionalization of Cdots for *in vivo* imaging and biosensors.

This work was supported by 973 Program (No. 2011CB707703), NSFC (No. 21375064 and 81301080), and Research Fund for the Doctoral Program of Higher Education (No. 20130031110016).

Notes and references

[a] State Key Laboratory of Medicinal Chemical Biology, Collaborative Innovation Center of Chemical Science and Engineering (Tianjin), and Research Center for Analytical Sciences, College of Chemistry, Nankai University, Tianjin, 300071, China.

[b] Key Laboratory of Animal Models and Degenerative Neurological Diseases (Tianjin), School of Medicine, Nankai University, Tianjin, 300071, China.

* Email: xbyin@nankai.edu.cn; Fax: +86-22-23503034.

† These authors contributed equally.

Electronic Supplementary Information (ESI) available: Experimental section, Fig. S1–S11 and Table S1-S2. See DOI: 10.1039/c000000x/

1. S. N. Baker and G. A. Baker, *Angew. Chem. Int. Ed.*, 2010, **49**, 6726-6744.
2. L. Cao, M. J. Meziani, S. Sahu and Y.-P. Sun, *Acc. Chem. Res.*, 2012, **46**, 171-180.
3. P. G. Luo, F. Yang, S.-T. Yang, S. K. Sonkar, L. Yang, J. J. Broglie, Y. Liu and Y.-P. Sun, *RSC Adv.*, 2014, **4**, 10791-10807.
4. W. Wei, C. Xu, L. Wu, J. Wang, J. Ren and X. Qu, *Sci. Rep.*, 2014, **4**.
5. J. Peng, W. Gao, B. K. Gupta, Z. Liu, R. Romero-Aburto, L. Ge, L. Song, L. B. Alemany, X. Zhan, G. Gao, S. A. Vithayathil, B. A. Kaipparettu, A. A. Marti, T. Hayashi, J.-J. Zhu and P. M. Ajayan, *Nano. Lett.*, 2012, **12**, 844-849.
6. V. N. Mochalin and Y. Gogotsi, *J. Am. Chem. Soc.*, 2009, **131**, 4594-4595.
7. C.-T. Chien, S.-S. Li, W.-J. Lai, Y.-C. Yeh, H.-A. Chen, I. S. Chen, L.-C. Chen, K.-H. Chen, T. Nemoto, S. Isoda, M. Chen, T. Fujita, G. Eda, H. Yamaguchi, M. Chhowalla and C.-W. Chen, *Angew. Chem. Int. Ed.*, 2012, **51**, 6662-6666.
8. S. K. Bhunia, A. Saha, A. R. Maity, S. C. Ray and N. R. Jana, *Sci. Rep.*, 2013, **3**.
9. Q.-Q. Shi, Y.-H. Li, Y. Xu, Y. Wang, X.-B. Yin, X.-W. He and Y.-K. Zhang, *RSC Adv.*, 2014, **4**, 1563-1566.
10. S. Zhu, Q. Meng, L. Wang, J. Zhang, Y. Song, H. Jin, K. Zhang, H. Sun, H. Wang and B. Yang, *Angew. Chem. Int. Ed.*, 2013, **52**, 3953-3957.
11. J. Zhou, Y. Yang and C.-y. Zhang, *Chem. Commun.*, 2013, **49**, 8605-8607.
12. Z. Qian, J. Ma, X. Shan, H. Feng, L. Shao and J. Chen, *Chem. Eur. J.*, 2014, **20**, 2983-2983.
13. Z. L. Wu, P. Zhang, M. X. Gao, C. F. Liu, W. Wang, F. Leng and C. Z. Huang, *J. Mater. Chem. B*, 2013, **1**, 2868-2873.
14. Q. Liu, B. Guo, Z. Rao, B. Zhang and J. R. Gong, *Nano. Lett.*, 2013, **13**, 2436-2441.
15. M. Xu, G. He, Z. Li, F. He, F. Gao, Y. Su, L. Zhang, Z. Yang and Y. Zhang, *Nanoscale*, 2014, **6**, 10307-10315.
16. Q. L. Zhao, Z. L. Zhang, B. H. Huang, J. Peng, M. Zhang and D. W. Pang, *Chem. Commun.*, 2008, 5116-5118.
17. H. P. Liu, T. Ye and C. D. Mao, *Angew. Chem. Int. Ed.*, 2007, **46**, 6473-6475.
18. Y. Xu, M. Wu, Y. Liu, X.-Z. Feng, X.-B. Yin, X.-W. He and Y.-K. Zhang, *Chem. Eur. J.*, 2013, **19**, 2276-2283.
19. Y. Xu, M. Wu, X.-Z. Feng, X.-B. Yin, X.-W. He and Y.-K. Zhang, *Chem. Eur. J.*, 2013, **19**, 6282-6288.
20. X. Xu, R. Ray, Y. Gu, H. J. Ploehn, L. Gearheart, K. Raker and W. A. Scrivens, *J. Am. Chem. Soc.*, 2004, **126**, 12736-12737.
21. S. Mitra, S. Chandra, T. Kundu, R. Banerjee, P. Pramanik and A. Goswami, *RSC Adv.*, 2012, **2**, 12129-12131.
22. C. J. Liu, P. Zhang, X. Y. Zhai, F. Tian, W. C. Li, J. H. Yang, Y. Liu, H. B. Wang, W. Wang and W. G. Liu, *Biomaterials*, 2012, **33**, 3604-3613.
23. J. Jiang, Y. He, S. Y. Li and H. Cui, *Chem. Commun.*, 2012, **48**, 9634-9636.
24. C. Ding, A. Zhu and Y. Tian, *Acc. Chem. Res.*, 2014, **47**, 20-30.
25. H.-T. Sun, J. Yang, M. Fujii, Y. Sakka, Y. Zhu, T. Asahara, N. Shirahata, M. Ii, Z. Bai, J.-G. Li and H. Gao, *Small*, 2011, **7**, 199-203.
26. Y.-Y. Zhang, M. Wu, Y.-Q. Wang, X.-W. He, W.-Y. Li and X.-Z. Feng, *Talanta*, 2013, **117**, 196-202.
27. S. Chandra, P. Das, S. Bag, D. Laha and P. Pramanik, *Nanoscale*, 2011, **3**, 1533-1540.
28. X. Wang, K. Qu, B. Xu, J. Ren and X. Qu, *J. Mater. Chem.*, 2011, **21**, 2445-2450.
29. X. Zhai, P. Zhang, C. Liu, T. Bai, W. Li, L. Dai and W. Liu, *Chem. Commun.*, 2012, **48**, 7955-7957.
30. Z. Qian, J. Ma, X. Shan, L. Shao, J. Zhou, J. Chen and H. Feng, *RSC Adv.*, 2013, **3**, 14571-14579.
31. J. G. Zhou, C. Booker, R. Y. Li, X. T. Zhou, T. K. Sham, X. L. Sun and Z. F. Ding, *J. Am. Chem. Soc.*, 2007, **129**, 744-745.
32. Y. P. Sun, B. Zhou, Y. Lin, W. Wang, K. A. S. Fernando, P. Pathak, M. J. Meziani, B. A. Harruff, X. Wang, H. F. Wang, P. J. G. Luo, H. Yang, M. E. Kose, B. L. Chen, L. M. Veca and S. Y. Xie, *J. Am. Chem. Soc.*, 2006, **128**, 7756-7757.
33. S. J. Zhu, J. H. Zhang, C. Y. Qiao, S. J. Tang, Y. F. Li, W. J. Yuan, B. Li, L. Tian, F. Liu, R. Hu, H. N. Gao, H. T. Wei, H. Zhang, H. C. Sun and B. Yang, *Chem. Commun.*, 2011, **47**, 6858-6860.

34. Y. Li, Y. Zhao, H. Cheng, Y. Hu, G. Shi, L. Dai and L. Qu, *J. Am. Chem. Soc.*, 2011, **134**, 15-18.
35. Y. Dong, J. Shao, C. Chen, H. Li, R. Wang, Y. Chi, X. Lin and G. Chen, *Carbon*, 2012, **50**, 4738-4743.
36. G. J. Lieschke and P. D. Currie, *Nat. Rev. Genet.*, 2007, **8**, 353-367.
37. S. K. Ko, X. Chen, J. Yoon and I. Shin, *Chem. Soc. Rev.*, 2011, **40**, 2120-2130.
38. S. T. Laughlin, J. M. Baskin, S. L. Amacher and C. R. Bertozzi, *Science*, 2008, **320**, 664-667.
39. J. M. Baskin, K. W. Dehnert, S. T. Laughlin, S. L. Amacher and C. R. Bertozzi, *Proc. Natl. Acad. Sci.*, 2010, **107**, 10360-10365.
40. S. A. Brittijn, S. J. Duivesteijn, M. Belmamoune, L. F. M. Bertens, W. Bitter, J. D. Debruijn, D. L. Champagne, E. Cuppen, G. Flik, C. M. Vandenbroucke-Grauls, R. A. J. Janssen, I. M. L. de Jong, E. R. de Kloet, A. Kros, A. H. Meijer, J. R. Metz, A. M. van der Sar, M. J. M. Schaaf, S. Schulte-Merker, H. P. Spaink, P. P. Tak, F. J. Verbeek, M. J. Vervoordeldonk, F. J. Vonk, F. Witte, H. Yuan and M. K. Richardson, *Int. J. Dev. Biol.*, 2009, **53**, 835-850.
41. M. Wu, Z. W. Yu, Y. Liu, D. F. Feng, J. J. Yang, X. B. Yin, T. Zhang, D. Y. Chen, T. J. Liu and X. Z. Feng, *ChemBioChem*, 2013, **14**, 979-986.
42. Y. F. Huang, X. Zhou, R. Zhou, H. Zhang, K. B. Kang, M. Zhao, Y. Peng, Q. Wang, H. L. Zhang and W. Y. Qiu, *Chem. Eur. J.*, 2014, **20**, 5640-5648.
43. J. J. Herman, R. Radin and R. Schneiderman, *J. Pediatr.*, 1983, **102**, 196-199.
44. Y. Mine, *Trends. Food. Sci. Tech.*, 1995, **6**, 225-232.
45. S. Guo and S. Dong, *J. Mater. Chem.*, 2011, **21**, 18503-18516.
46. X.-Y. Wang, A. Gao, C.-C. Lu, X.-W. He and X.-B. Yin, *Biosens. Bioelectron.*, 2013, **48**, 120-125.
47. J.-L. Chen, X.-P. Yan, K. Meng and S.-F. Wang, *Anal. Chem.*, 2011, **83**, 8787-8793.
48. M. Li, X. Zhou, S. Guo and N. Wu, *Biosens. Bioelectron.*, 2013, **43**, 69-74.